Silencing lncRNA HOTAIR improves the recovery of neurological function in ischemic stroke via the miR-148a-3p/KLF6 axis

Yiwen Huang
Guangzhou First People's Hospital, School of Medicine, South China University of Technology
Yuanyuan Wang
Guangzhou First People's Hospital, School of Medicine, South China University of Technology
Xiaobin Liu
Guangzhou First People's Hospital, School of Medicine, South China University of Technology
Yingjun Ouyang (yingjunoy0728@163.com)
Guangzhou First People's Hospital, School of Medicine, South China University of Technology

Research Article

Keywords: Ischemic stroke, LncRNA HOTAIR, microRNA-148a-3p, KLF6, Neurological function recovery, STAT3 signaling pathway, Apoptosis, Inflammation

Posted Date: March 13th, 2021

DOI: https://doi.org/10.21203/rs.3.rs-287212/v1

Abstract

Ischemic stroke (IS), caused by a permanent or transient local reduction in blood supply to the brain, is one of the most widespread causes of public health problems in modern society. Long non-coding RNA (LncRNA) has been reported to be related to angiogenesis following IS. In this study, we explored the effect and potential molecular mechanism of lncRNA HOTAIR in IS. Permanent middle cerebral artery occlusion (pMCAO) model and oxygen and glucose deprivation (OGD) model were established. HOTAIR was increased *in vivo* and *in vitro* models post-ischemic. HOTAIR knockdown promoted neurological function recovery, manifesting in decreased modified neurological severity score, cerebral infarcted area, apoptosis and inflammation, and improved balance ability, spatial learning and memory ability. Silencing HOTAIR also improved the viability of OGD-induced N2a cells, and attenuated apoptosis and inflammation. HOTAIR can compete with KLF6 to bind to miR-148a-3p. miR-148a-3p knockdown or KLF6 overexpression partially reversed the effect of sh-HOTAIR on OGD-induced N2a cells. HOTAIR suppressed the activation of STAT3 pathway via the miR-148a-3p/KLF6 axis. To summarize, this study demonstrated that lncRNA HOTAIR absorbed miR-148a-3p and up-regulate KLF6 expression through ceRNA mechanism, and inhibited STAT3 pathway, promoted apoptosis and inflammation, and aggravated neurological injury post-IS.

Introduction

Stroke is one of the leading causes of mortality and disability around the world and ischemic stroke (IS) takes up about 87% of all strokes [1]. It occurs when brain blood flow stops and then leads to reduced supply of oxygen and glucose to cells in the brain [2]. The patients of IS can display neurological impairment such as paralysis, language disorders, facial and limb incoordination [3]. Various risk factors, including high blood pressure, diabetes mellitus, obesity, high blood cholesterol, smoking, atrial fibrillation, and previous transient ischemic attack, are involved in IS [4]. However, current measures to protect the brain against IS are still insufficient [5]. Therefore, an underlying mechanism of cerebral ischemic injury is urgently needed.

Long-non-coding RNA (LncRNA) is a transcript of RNA with a length of over 200 nucleotides but without an open reading framework [6]. LncRNAs play important roles in regulating the expression level of protein-coding genes and related signaling pathways involved in development of multiple diseases [7]. Study has reported that lncRNAs are involved in IS and mediate ischemic neuronal death in stroke [8]. LncRNAs homeobox antisense non-coding RNA (HOTAIR) has been reported to promote ischemic infarct induced by hypoxia [9]. Study has reported that HOTAIR aggravates H_2O_2-induced injury in cardiomyocytes and exacerbates myocardial ischemia-reperfusion (I/R) injury [10]. Evidence has confirmed that lncRNAs act as competing endogenous RNAs (ceRNAs) by competing for binding to microRNAs (miRs) [11]. It has been reported that HOTAIR acts as a ceRNA for miR-126-5p to modulate rab3a interacting protein expression in Parkinson's disease [12]. But the ceRNA network of HOTAIR in IS is elusive.

miRs are small, endogenous, single-stranded, non-coding RNA molecules ranging in length from 18–25 nt [13]. Previous study has demonstrated that miRs contribute to IS pathogenesis, and miRs participate in the pathogenesis of ischemic brain injury in rodent stroke models [14]. In patients with acute IS, miR-148a was decreased [15]. miR-148a also protects murine liver from alleviates hepatic I/R injury [16]. Furthermore, miR-148a-3p participates in oxidative stress injury induced by I/R [17]. But, the role of miR-148a-3p in IS has not been investigated yet.

Whether HOTAIR can affect miR-148a-3p and participate in the neurological recovery in IS is largely unknown. And there is no report concerning this research topic at home and abroad. To address this gap in knowledge, in this work, we investigated the role of HOTAIR in the neurological recovery in IS and explored the potential molecular mechanism.

Material And Methods

Ethic statement

All experiments were authorized by the Ethical Committee of Guangzhou First People's Hospital, School of Medicine, South China University of Technology.
The animal experiments were conducted following the guidelines for the care and use of laboratory animals.
All procedures were strictly implemented by the code of ethics.

Establishment and grouping of permanent middle cerebral artery occlusion (pMCAO) mice

A total of 96 adult male C57BL/6 mice (6–8 weeks, 20–28 g) were purchased from Vital River Laboratory Animal Technology [SYXK (Beijing) 2017-0033, Beijing, China]. The mice were placed in separate cages at 22°C ± 2°C and 65 ± 5% relative humidity on a 12 h light/12 h dark cycle with free access to food and water.

The pMCAO mouse model was established [18]. Mice were anesthetized with 2% pentobarbital sodium (50 mg/kg) (Sigma Chemical Co., St. Louis, MO, USA) by intraperitoneal injection. The right common carotid artery (CCA) was exposed and ligated using (5/0) surgical suture through a ventral midline neck incision. Mice were placed in left lateral decubitus position. An incision was made from the lateral orbit to the external auditory meatus, the base the parotid gland and the upper part of the temporal muscle were isolated to expose the cortical branches of middle cerebral artery (MCA) under the right side of skull. A craniotomy was performed directly above the distal part of the MCA using a 0.8 mm high-speed micro drill. Coagulator was used to cauterize the exposed cortical branches of MCA on the right side of the brain. The operation should be performed with caution to avoid damage to the surrounding brain tissue. The incision was sutured using conventional method. Mice should be kept warm during operation. The sham-operated mice only received the separation of cervical vessels and exposure of skull and drilling holes without ligation of right CCA and cauterization of corresponding arteries. The neurological function score and cerebral infarct area were analyzed 24 h after model establishment.

Mice were randomly assigned into 4 groups (N = 24 in each group): sham group, pMCAO group, pMCAO + sh-HOTAIR group, and pMCAO + sh-NC group. The low expression lentivirus shRNA HOTAIR (sh-HOTAIR) and its control (sh-NC) were constructed and packaged by GenePharma (Shanghai, China). Lentivirus processing was applied 2 weeks before pMCAO operation. Mice were anesthetized and fixed in a stereotactic apparatus (RWD Life Science Co., Ltd, Shenzhen, China). The lentivirus was injected via the right lateral ventricle at the following coordinates: 0.3 mm posterior to bregma, 1 mm right lateral to sagittal suture, 2.2 mm deep to the dura. The 5 μL lentivirus was slowly injected at a rate of 1 μL/min using a Hamilton microinjector, and the needle was retained in place for 5 min following the injection. The titer for sh-HOTAIR and its control were 3×10^8 CFU/mL [19].

Neurobehavioral evaluation

Mice were evaluated for neurological function after 24 h of pMCAO modeling based on the modified neurological severity score (mNSS) [20] in a double blind manner from perspectives of movement, sensation and reflex. Evaluation standards were: motor tests (1–9 points) including raising mice by the tail, placing mice on the floor and abnormal movement; sensory tests (1–2 points) including placing test (visual and tactile test) and proprioceptive test; reflex tests (1–3 points) including pupil reflex, corneal reflex and startle reflex. The mNSS score was divided into: minor injury (1–4 points), moderate injury (5–9 points) and severe injury (10–14 points). Higher score meant severer deficit.

Beam balance test

Beam balance test was applied to observe the ability of coordinating muscles and keeping balance of mice [20]. The wooden beam (length 1 m, width 5 mm, diameter 15 mm, horizontally positioned 1 m above the underlying surface) was supported by platforms at both sides. The mouse was placed at the start of the beam and scored based on its performance on the beam. The three-day trial was performed twice a day with a 5 min interval. The average value was taken as the experiment result. Performance on each trial was scored as follows: reach the platform or balance in steady posture, 0 point; grasp one side of the beam, 1 point; hang the beam and one limb falls off the beam, 2 points; hang the beam and two limbs fall off the beam or rotate on the beam for over 60 s, 3 points; try to keep balance on the beam for over 40 s but fall, 4 points; try to keep balance on the beam for over 20 s but fall, 5 points; fall with no intention to keep balance, 6 points. Higher score meant worse balance ability.

Morris water maze test

Water maze test was applied to evaluate the learning-memory, spatial location and orientation capability of mice [21]. Titanium dioxide (Shanghai Jianghu Titanium Dioxide Chemical Industry Co., Ltd, Shanghai, China) was added into the water at concentration of 125 g/L. Morris water maze system (Mobile Datum, Shanghai, China) was applied for animal behavior analysis and water temperature was kept at 25°C. The tests included two parts: orientation navigation experiment and space exploration experiment. In the orientation navigation experiment, mice were placed in the water and the time (s) to find the platform was recorded (escape latent period). If the mice were unable to find the platform within 60 s, the experimenter guided the mice to the platform and time was recorded as 60 s. Each mouse was trained for 4 times per day with 15–20 min interval for 4 days. In the space exploration experiment, on day 5, the platform was

removed. Mice were placed in the water randomly and swam for 60 s. The time of the mice crossing the original platform was recorded.

2,3,5-triphenyltetrazolium chloride (TTC) staining

Mice were euthanized by injection of 800 mg/kg pentobarbital sodium after beam balance test. Brain was taken out and made into continuous slices at 2 mm. The slices were incubated in 2% TTC solution (2530-85-0, Guidechem, Shanghai, China) at 37°C in the dark for 30 min. Normal brain tissues showed a pink or red color, and infarcted tissues were in light grey. TTC-stained slices were photographed using a digital camera. The cerebral infarcted area was calculated using Image J (National Institutes of Health, Bethesda, MD, USA) software.

TdT-mediated dUTP Nick-End Labeling (TUNEL)

The brain tissues were cut into sections at 5 μm and dewaxed by xylene and dehydrated with ethanol, and treated according to the instructions of TUNEL kit (C1089, Beyotime, Shanghai, China). Briefly, 20 μg/mL protease K working solution (Solarbio, Beijing, China) was added at room temperature for 15 min. The sections were washed using phosphate buffered saline (PBS) for 3 times, and then added with 50 μL TUNEL detection solution and incubated in the dark for 60 min. After being washed by PBS for 3 times, the samples were added with primary antibody NeuN (ab177487, Abcam Inc., Cambridge, MA, USA) and the Alexa Fluor® 488-labeled secondary antibody (ab150077, Abcam). Then sections were counterstained using 4,6-diamidino-2-phenylin-dole (DAPI). The images were obtained by a fluorescence microscope (Leica, Wetzlar, Germany). The apoptosis rate = apoptotic cells (red)/total cells (blue)∗100%.

Oxygen–glucose deprivation (OGD) model establishment

N2a cells (ATCC, Manassas, VA, USA) were cultured in Dulbecco's modified Eagle's medium (DMEM) (A4192101, Gibco, Grand Island, NY, USA) + 10% fetal bovine serum (FBS) (Thermo Fisher Scientific, Shanghai, China) in 5% CO_2 incubator at 37°C.

The *in vitro* OGD model was established as previously described [22]. Cells in good growth conditions were cultured in glucose, serum and oxygen free DMEM with 95% N_2 and 5% CO_2 at 37°C for 3 h. The cells were washed with PBS and then added with 10% FBS high glucose medium and cultured with 5% CO_2 at 37°C for the following experiments.

The design and synthesis of miR-148a-3p inhibitor, inhibitor NC and pcDNA3.1-KLF6, and pcDNA3.1-NC were processed by RiboBio Company (Guangzhou, China). The cells were transferred in accordance with the instructions of Lipofectamine 3000 (Thermo Fisher Scientific). For HOTAIR lentivirus treatment, cells in plates at a density of 5×10^6 cells/well were cultured for 24 h and then cultured in 2 mL fresh complete medium containing 10ug/mL polybrene for 1h at 37°C. Then 15 mL lentivirus with a multiplicity of infection (MOI) of 30 was added to the cell suspension and incubated for 6 h. The medium was then replaced with equal volume of fresh medium again and the cells were incubated for further experiments [23]. Cells were assigned into normal, OGD, OGD + sh-NC, OGD + sh-HOTAIR, OGD + sh-HOTAIR + inhibitor NC (sh-HOTAIR + inhibitor NC), OGD + sh-HOTAIR + miR-148a-3p inhibitor (sh-HOTAIR + inhibitor), OGD + sh-

HOTAIR + pcDNA3.1 NC (sh-HOTAIR + pcDNA-NC), OGD + sh-HOTAIR + pcDNA3.1-KLF6 (sh-HOTAIR + pcDNA-KLF6).

Cell counting kit-8 (CCK-8) assay

Cells from each group were extracted and made into single cell suspension and seeded in 96-well plates (1×10^4 cells/well) with 100 μL per well for 24 h. CCK-8 solution (Dojindo Molecular Technologies, Kumamoto, Japan) was added (10 μL/well) into each well, and the cells were incubated for 2 h at 37°C in a 5% CO_2 incubator. The absorbance was detected using an EnVision multimode plate reader (Plate Reader, PerkinElmer, Waltham, MA, USA) at 450 nm and relative cell viability was calculated.

Flow cytometry

The cells were detached by trypsin. A total of 1×10^5 cells/mL suspended cells were harvested and detected using Annexin V-FITC cell death detection kit (BD Bioscience, Franklin Lakes, NJ, USA). First, 100 μL 1× Annexin buffer was used to suspend cells. Then 5 μL Annexin V-FITC and 1 μL propidium iodide were added to stain the cells for 15 min at 4°C without light exposure. Apoptosis was then detected on a flow cytometer (FACScan, BD Biosciences).

Fractionation of nuclear and cytoplasmic RNA

The PARIS™ kit (#AM1921, Thermo Fisher Scientific) was applied for fractionation of nuclear and cytoplasmic RNA to detect expression of lncRNA HOTAIR in nucleus and cytoplasm of mouse N2a cells. The expression of HOTAIR was analyzed by RT-qPCR.

Florescence in situ hybridization (FISH)

Firstly, online software LncATLAS (http://lncatlas.crg.eu/) was applied to predict the distribution of HOTAIR. Then, FITC-labeled HOTAIR was designed and synthesized by GenePharma. Nuclei were stained with DAPI. All processes were conducted using the FISH kit (GenePharma) following the manufacturer's instructions. Images were obtained by a FV3000 microscope (Olympus, Tokyo, Japan).

Bioinformatics analyses

HOTAIR related miRs were retrieved using starBase database (starbase.sysu.edu.cn/) and RAID database (http://www.rna-society.org/raid2/index.html). IS expression chip GSE35338 of mouse samples was obtained through GEO database (https://www. ncbi.nlm.nih.gov/geo/), including 10 normal samples and 11 disease samples. The "limma" package in R language was used for differential analysis. False discovery rate (FDR) was used to rectify *P* value, and differentially expressed genes from IS mouse model were screened out with |logFC|>1 and adj.p.val < 0.05 as criteria. The miR-148q-3p target gene in human and mice was predicted using TargetScan database (http://www.targetscan.org/vert_71/) and binding sites were obtained. Interaction analysis of 11 candidate genes was performed using GeneMANIA database (http://genemania.org/), and then interaction scores were obtained.

Dual-luciferase reporter assay

The potential binding sites of lncRNA HOTAIR and miR-148a-3p were predicted using RNA22 v2 (https://cm.jefferson.edu/rna22/Interactive/) [24]. The potential binding sites of miR-148a-3p and kruppel-

like factor 6 (KLF6) were predicted using starBase (http://starbase.sysu.edu.cn/index.php) [25]. The wild type (wt) and mutant type (mut) sequences of HOTAIR and KLF6 were cloned to pmiR-GLO luciferase vector (Promega, Madison, WI, USA) to construct HOTAIR-wt, KLF6-wt and HOTAIR-mut and KLF6-mut. HEK293T cells (Shanghai Institute of Biochemistry and Cell Biology, Chinese Academy of Sciences, Shanghai, China) were transferred with the constructed plasmids and mimic NC and miR-148a-3p mimic (GenePharma), respectively using lipofectamine 3000 (Thermo Fisher Scientific). Luciferase activity was detected after 48 h by the Dual-Luciferase Reporter Assay kit (Vazyme, Nanjing, China) following the manufacturer's instructions.

RNA pull-down

The biotinylated mut or wt miR-148a-3p (GenePharma) or its negative control (NC-bio) was transfected into the cells. The cells were lysed using lysis buffer at 48 h post-transfection. Then, streptavidin agarose beads (Invitrogen, Carlsbad, CA, USA) were incubated with the cell lysates, and the RNA complex that bound to the beads was eluted and purified using TRIzol reagent (Takara, Shiga, Japan). Gene level in the RNA complex was analyzed by RT-qPCR [26].

Enzyme-linked immunosorbent assay (ELISA)

The homogenate or cell suspension from each group was centrifuged at 4°C for 10 min at 1,000 g and the supernatants were collected. Protein contents of tumor necrosis factor-α (TNF-α) (MTA00B), interleukin (IL)-6 (M6000B) and IL-10 (M1000B) were measured using ELISA kits (R&D Systems, Minneapolis, MN, USA).

RT-qPCR

Total RNA and miRs were extracted separately from mice brain tissues and cells with TRIzol reagent and miRNeasy Mini Kit (Invitrogen). cDNA was synthetized using M-MLV reverse transcriptase (Invitrogen) or TaqMan MicroRNA Reverse Transcription Kit (Thermo Fisher Scientific). RT-qPCR was performed using SYBR Green Real-Time PCR Master Mix (Thermo Fisher Scientific) or TaqMan miRNA assay kit on Applied Biosystems7900 Real-Time PCR System. GAPDH and U6 were used as internal controls. Relative expression levels were calculated using the $2^{-\triangle\triangle ct}$ method. Amplified primer sequences are illustrated in Table 1.

Table 1
Primer sequences

Gene	Forward 5’-3’	Reverse 5’-3’
LncRNA HOTAIR	CAGGACGCTGTTCTTGTTGA	CGGAACAGCTACTCCTCCTG
miR-148a-3p	TCAGTGCACTACAGAA	CAGTGCGTGTCGTGGAGT
KLF6	ATGAAACTTTCACCTGCGCT	TCAGAGGTGCCTCTTCATGT
U6	CGCTTCGGCAGCACATATAC	AAATATGGAACGCTTCACGA
GAPDH	ATGGCGTAGCAATCTCCT	TTACTCCTTGGAGGCCAT

Note: LncRNA HOTAIR, long-non-coding RNA HOX transcript antisense intergenic RNA; miR, microRNA; KLF6, kruppel-like factor 6; GAPDH, glyceraldehyde-3-phosphate dehydrogenase.

Western blot

Total proteins from homogenate and cells were extracted with radio immunoprecipitation assay (RIPA) lysates (Beyotime). Proteins were quantitatively detected by a bicinchoninic acid kit (Thermo Fisher Scientific). Extracted protein was denatured at 100°C for 5 min. A total of 50–100 μg protein was separated by sodium dodecyl sulfate-polyacrylamide gel (SDS-PAGE), and then proteins were transferred onto polyvinylidene fluoride (PVDF) membranes and incubated with 5% skim milk for 2 h, followed by Tris-buffered saline Tween (TBST) washing for 3 times. The primary antibody p-STAT3 (1:20000, ab76315, Abcam) or GAPDH (1:1000, ab9485, Abcam) was added and the membranes were incubated overnight at 4°C. After washing in TBST, the secondary antibody Goat Anti-Rabbit IgG H&L (HRP) (1:5000, ab97051, Abcam) was added and the membranes were incubated for 2 h at 37°C and detected using chemiluminescent method. Grey value analysis was performed using Image J (National Institutes of Health).

Statistical analysis

Data analysis and drafting were performed using SPSS 21.0 software (IBM Corp. Armonk, NY, USA) and GraphPad Prism8.0.1 (GraphPad Software Inc., San Diego, CA, USA). Data were in normal distribution and presented as mean ± standard deviation (SD). Differences between groups were analyzed using one-way analysis of variance (ANOVA) or two-way ANOVA, followed by Tukey's multiple comparisons test or Sidak's multiple comparisons test. P value was obtained using a two-sided test. $P < 0.05$ was considered a statistically significant difference.

Results

LncRNA HOTAIR inhibited recovery of neurological function in pMCAO mice

IS is attributed to an abrupt reduction of cerebral blood flow, resulting in hypoxia that triggers neuroinflammation, which could result in disability and even death [27]. LncRNAs play critical roles in occurrence and development of IS [1]. In order to explore the function of lncRNA in IS, lncRNAs related to IS were retrieved in LncDisease database (http://www.rnanut.net/lncrnadisease) [28] (Fig. 1A) and finally 2 candidate lncRNAs were obtained. The role of HOTAIR in the recovery of neurological function in IS is still not clear. To further investigate the role of HOTAIR, pMCAO mouse model was established first, and neurological score was assessed using mNSS method. The pMCAO mice developed severe neurological deficit. The beam balance test suggested that pMCAO mice had poor ability to maintain balance. The escape latency in water maze test was obviously increased and the times crossing the platform were significantly decreased (Fig. 1B-D, $P < 0.01$). These results indicated the success in pMCAO mouse model.

Subsequently, the expression of HOTAIR in cerebral tissues at 24 h after pMCAO model establishment was detected by RT-qPCR. The result indicated that the expression of HOTAIR in pMCAO mice was increased significantly. Then, lentivirus was injected to the mice to silence HOTAIR expression. The result showed that the expression of HOTAIR was decreased significantly using the shRNA HOTAIR (Fig. 1E, $P < 0.01$). The scores of neurological deficits and motor balance were decreased in mice with silencing HOTAIR, along with decreased escape latency and increased platform crossing times (Fig. 1B-D, all $P < 0.01$). In addition, the infarcted area in pMCAO mice was increased significantly, accompanied with increased apoptosis of neural cells, which were decreased after lowering HOTAIR expression (Fig. 1F-G, all $P < 0.01$). Inflammation in cerebral tissues contributes to brain injury in IS [29, 30]. Therefore, we examined the influence of HOTAIR on inflammation in pMCAO mice and found that levels of TNF-α and IL-6 were increased while IL-10 level was decreased; but levels of TNF-α and IL-6 were decreased, and IL-10 level was increased in cerebral tissues with silencing HOTAIR (Fig. 1H, all $P < 0.01$). Above results demonstrated that silencing HOTAIR suppressed apoptosis and inflammation, attenuated neurobehavioral deficit and promoted the recovery of neurological function of pMCAO mice.

Silencing HOTAIR promoted viability of OGD-injured N2a cells and attenuated apoptosis and inflammation

We simulated IS *in vitro* using OGD-injured N2a cells to further investigate the role of HOTAIR in IS. The reduction of cell viability injured by OGD indicated the success in establishing OGD model (Fig. 2A, $P < 0.01$). The expression of HOTAIR was detected by RT-qPCR and the result showed that HOTAIR expression in ODG cells increased significantly. Then, we lowered the expression of HOTAIR in OGD cells using shRNA HOTAIR (Fig. 2B, $P < 0.01$), and silencing HOTAIR increased remarkably the cell viability (Fig. 2A, $P < 0.01$). Result of flow cytometry showed that apoptotic rate of OGD-induced cells was increased and silencing HOTAIR reduced apoptosis (Fig. 2C, $P < 0.01$). ELISA showed higher levels of TNF-α and IL-6 and lower level of IL-10 in OGD cells, and lower levels of TNF-α and IL-6 and higher level of IL-10 in cells with silencing HOTAIR expression (Fig. 2D, all $P < 0.01$). In conclusion, silencing HOTAIR promoted viability of OGD-induced neurons and attenuated apoptosis and inflammation

HOTAIR regulated KLF6 expression via targeting miR-148a-3p

Study has found that HOTAIR plays a regulatory role through ceRNA mechanism [31]. LncATLAS database (http://lncatlas.crg.eu/) predicted that HOTAIR was mainly located in the cytoplasm of N2a cells, which was also proved by the experiment results (Fig. 3A-B). The downstream miRs of HOTAIR were further predicted by RAID and starBase databases (Fig. 3C) and miR-148a-3p and miR-326 were obtained. It has been found that miR-148a-3p expression was low in cerebral I/R [17]. IS chip GSE35338 was retrieved in GEO database and differential analysis revealed that most genes were highly expressed in IS samples (Fig. 3D). Because the samples of GSE35338 chip were mice, therefore, we predicted downstream regulatory target genes of miR-148a-3p in both human and mice. Meanwhile, the significant up-regulated genes in GSE35338 chip were intersected and finally 11 candidate genes were obtained (Fig. 3E). Interaction analysis was performed to these candidate genes and interaction scores were gained (Fig. 3F-G, $P < 0.01$). The result showed the highest score in KLF6 (Supplementary Table 1). Also, KLF6 was highly expressed in IS chip GSE35338. Above results implied that lncRNA-HOTAIR may regulate IS progress through the miR-148a-3p/KLF6 axis. Next, the binding sites of HOTAIR and miR-148a-3p and that of miR-148a-3p and KLF6 (Fig. 3H) were predicted using RNA22 v2 (https://cm.jefferson.edu/rna22/Interactive/) [24] and starBase (http://starbase.sysu.edu.cn/index.php) [25]. The results of dual-luciferase assay and RNA pull-down experiment revealed the binding relation of HOTAIR and miR-148a-3p, and miR-148a-3p and KLF6 (Fig. 3I-J, $P < 0.01$). The expressions of miR-148a-3p and KLF6 were detected by RT-qPCR and the result showed that miR-148a-3p expression was decreased and KLF6 expression was increased after ischemia *in vivo* and *in vitro*. After inhibiting HOTAIR expression, miR-148a-3p expression was increased and KLF6 expression was decreased (Fig. 3K-L, $P < 0.01$). Above results indicated that HOTAIR regulated KLF6 expression via targeting miR-148a-3p.

miR-148a-3p downregulation partially reversed the effect of sh-HOTAIR on N2a cells post-ischemia

To explore the effect of miR-148a-3p, we transferred miR-148a-3p inhibitor to N2a cells with silencing HOTAIR expression and succeeded in lowering miR-148a-3p expression (Fig. 4A, $P < 0.01$). Then the cells were induced by OGD. The result of CCK-8 demonstrated that the viability of N2a cells in sh-HOTAIR + inhibitor group was decreased (Fig. 4B, all $P < 0.01$). Flow cytometry showed increased apoptotic rate after inhibiting miR-148a-3p expression (Fig. 4C, $P < 0.01$). The levels of TNF-α and IL-6 were increased and IL-10 level was decreased in sh-HOTAIR + inhibitor group (Fig. 4D, all $P < 0.01$). These findings revealed that miR-148a-3p downregulation reversed the effect of silencing HOTAIR on promoting N2a cell viability and attenuating apoptosis and inflammation.

KLF6 overexpression suppressed the effect of sh-HOTAIR on OGD-induced cell injury

To further verify the function of KLF6, we transferred pcDNA-KLF6 or pcDNA-NC into cells with silencing HOTAIR and then cells were treated by OGD to induce injury. RT-qPCR results demonstrated that the mRNA expression of KLF6 was upregulated (Fig. 5A, $P < 0.01$). Moreover, CCK-8 assay found that overexpression of KLF6 significantly repressed the viability of N2a cells (Fig. 5B, $P < 0.01$). Flow cytometry results revealed that overexpression of KLF6 led to the rising of apoptotic rate in N2a cells (Fig. 5C, $P < 0.01$). ELISA showed that overexpression of KLF6 caused increases in TNF-α and IL-6 levels and decrease in IL-10 level (Fig. 5D, $P < 0.01$). Taken together, these results demonstrated that

overexpression of KLF6 inhibited the viability of cells with silencing HOTAIR, increased apoptosis and aggravated inflammatory response.

HOTAIR blocked the activation of STAT3 signaling pathway via miR-148a-3p/KLF6

It has been reported that KLF6 inhibits the expression of anti-inflammatory genes by suppressing STAT3 signaling, which is involved in angiogenesis, neurogenesis and functional recovery after IS [32, 33]. We hypothesized that STAT3 signaling pathway may be involved in IS. Western blot was performed to detect the expression of p-STAT3 protein. The results demonstrated that the expression of p-STAT3 was decreased *in vivo* and *in vitro* ischemic models and silencing HOTAIR expression increased its expression while miR-148a-3p downregulation or overexpression of KLF6 reduced p-STAT3 expression (Fig. 6A-B, all $P < 0.01$). These results suggested that HOTAIR may affect the neurological injury in IS via the miR-148a-3p/KLF6 axis and the STAT3 signaling pathway.

Discussion

IS can result in a series of sequences, including cognitive impairment and epilepsy [34]. It has been suggested that lncRNAs may become a potential target for therapeutic intervention in ischemic brain injury [35]. In present study, we investigated the role of lncRNA HOTAIR/miR-148a-3p/KLF6 in the recovery of neurological function in IS.

After bioinformatics analysis, HOTAIR related to IS was selected as the focus of this study. We found HOTAIR was elevated in pMCAO mice. Then mice were injected with shRNA HOTAIR to silence HOTAIR expression to further explore HOTAIR action in pMCAO. Our study demonstrated that pMCAO mice displayed severe neurologic impairments including high scores of neurological deficits and motor balance, poor balance ability, prolonged escape latency and decreased platform crossing times. However, these neurologic impairments were reversed after lentivirus injection of shRNA HOTAIR. Inflammation and apoptosis play key roles in all stages of IS [34] and lncRNAs are suggested to be able to promote apoptosis and inflammation [1, 36]. The infarcted area, inflammation and apoptosis in pMCAO mice were also decreased significantly after silencing HOTAIR. The result is consistent with the recent researches that HOTAIR promotes neuroinflammation [36] and apoptosis cells [9]. Therefore, silencing HOTAIR suppressed apoptosis and inflammation, attenuated neurobehavioral deficit and promoted the recovery of neurological function of pMCAO mice. Lin et al. have also demonstrated that knockdown of HOTAIR expression reduced the apoptosis rate among dopamine neurons [12]. We then simulated IS *in vitro* using OGD-injured N2a cells to further investigate the role of HOTAIR in IS. HOTAIR expression in ODG cells was increased significantly. Then, we lowered the expression of HOTAIR in OGD cells using shRNA HOTAIR. Silencing HOTAIR remarkably promoted the cell viability, reduced apoptosis and levels of TNF-α and IL-6 and increased IL-10 level. Knocking down HOTAIR can facilitate cell viability and attenuate apoptosis [37]. The anti-inflammatory ability of shRNA HOTAIR has been identified in several studies [38–40]. The results above revealed that silencing HOTAIR promoted viability of OGD-injured N2a cell, and attenuated apoptosis and inflammation.

Study suggested that HOTAIR may act as a ceRNA to impose post-transcriptional regulation [41]. The experiment results identified that HOTAIR was located in the cytoplasm of N2a cells. The downstream miRs of HOTAIR were further predicted and then miR-148a-3p and miR-326 were obtained. miR-148a-3p was selected because it was poorly expressed in cerebral I/R [17]. IS chip GSE35338 analysis revealed that most genes were highly expressed in IS samples. Meanwhile, the significant upregulated genes were intersected and interaction analysis was performed. The result showed the highest score in KLF6. Also, KLF6 was highly expressed in IS chip GSE35338. Above results implied that lncRNA-HOTAIR may regulate IS progress through the miR-148a-3p/KLF6 axis. Moreover, the binding relations of HOTAIR and miR-148a-3p and that of miR-148a-3p and KLF6 were confirmed by dual-luciferase assay. Thereby, our research demonstrated that HOTAIR regulated KLF6 expression via targeting miR-148a-3p.

To explore the effect of miR-148a-3p, we transferred miR-148a-3p inhibitor into N2a cells with silencing HOTAIR and then induced cells by OGD. Our data elicited that the viability of OGD-induced N2a cells was reduced remarkably after inhibiting miR-148a-3p, apoptotic rate was increased, and the levels of TNF-α and IL-6 were increased and IL-10 level was decreased. As a novel repressor of inflammatory gene expression, miR-148a-3p plays a vital role in many diseases [42]. Previous investigation showed that miR-148a can alleviate hepatic I/R injury in mice [43]. Collectively, our study demonstrated that miR-148a-3p knockdown reversed the effect of sh-HOTAIR on OGD-induced N2a cells.

KLF6 is important in modulating inflammation and immune responses [44]. To further investigate the effect of KLF6, we transferred pcDNA-KLF6 into cells with silencing HOTAIR and then cells were treated by OGD to induce injury. The viability of OGD-induced N2a cells was decreased after overexpressing KLF6, apoptotic rate was obviously increased and levels of TNF-α and IL-6 were increased and level of IL-10 was decreased. Zhang et al. found that KLF6 exacerbates renal tubular epithelial cell damage and aggravates the inflammatory response in renal I/R injury [45]. Furthermore, KLF6 promotes macrophage inflammatory and hypoxia response [46]. In short, KLF6 overexpression repressed the viability of sh-HOTAIR-treated cells, and aggravated apoptosis and inflammatory response.

Besides, functional synergy of KLF6 and STAT3 has been clarified in central nervous system neurons [47]. One recent study has found that the activation of STAT3 pathway promotes microglia/macrophage polarization toward anti-inflammatory phenotype [48]. Our experiment result suggested that the expression of p-STAT3 was decreased *in vivo* and *in vitro* ischemic model, while silencing HOTAIR increased p-STAT3 expression, and miR-148a-3p knockdown or overexpression of KLF6 reduced its expression. Activating JAK2/STAT3 pathway is involved in the protection against cerebral I/R injury, and enhances cerebral angiogenesis and promotes neurological recovery after IS [49]. Taken together, HOTAIR affected neurological injury in IS through inhibition of STAT3 pathway mediated by the miR-148a-3p/KLF6 axis.

In conclusion, our study found that lncRNA HOTAIR inhibited STAT3 pathway and the recovery of neurological function in IS via the miR-148a-3p/KLF6 axis. Limitations still exist in the present study. Whether KLF6 can regulate neurological recovery through the STAT3 pathway, and whether HOTAIR and

miR-148a-3p can become biomarkers and potential therapeutic targets for the diagnosis and prognosis of IS require further investigations. The focus of future researches can be placed on the regulating mechanism of HOTAIR on miR-148a-3p/KLF6 from the view of epigenetics. It's reported that HOTAIR epigenetically can suppress miR-122 expression in hepatocellular carcinoma via DNA methylation [50]. But the regulating mechanism and biological functions between HOTAIR and DNA methylation in IS remain unclear. Moreover, the studies are rare in the involvement of lncRNA CDKN2B-AS1 and miR-326 in neurological recovery in IS. Therefore, the next step can be taken from this perspective.

Declarations

Data Availability

All the data generated or analyzed during this study are included in this published article.

Acknowledgements

Not applicable.

Funding

This study was supported by Guangzhou Science and Technology Planning Project (2060404).The funding body didn't participate in the design of the study and collection, analysis, and interpretation of data and in writing the manuscript.

Authors' contributions

YWH and YJOY are the guarantor of integrity of the entire study; YWH and YJOY contributed to study concepts and study design; YWH and YYW contributed to definition of intellectual content, literature research, clinical studies, experimental studies, manuscript preparation, manuscript editing, and manuscript review. YWH, YYW and XBL contributed to data acquisition, data analysis, and statistical analysis, All authors read and approved the final manuscript.

Conflict of Interest

The authors declare that they have no conflicts of interest.

ARRIVE guidelines

The authors confirmed that the study was carried out in compliance with the ARRIVE guidelines

References

1. Bao MH, Szeto V, Yang BB, Zhu SZ, Sun HS,Feng ZP. Long non-coding RNAs in ischemic stroke. *Cell Death Dis* **9**, 281. http://doi.10.1038/s41419-018-0282-x 2018.

2. Wang SW, Liu Z,Shi ZS. Non-Coding RNA in Acute Ischemic Stroke: Mechanisms, Biomarkers and Therapeutic Targets. *Cell Transplant* **27**, 1763-1777. http://doi.10.1177/0963689718806818 2018.
3. Balch MHH, Nimjee SM, Rink C,Hannawi Y. Beyond the Brain: The Systemic Pathophysiological Response to Acute Ischemic Stroke. *J Stroke* **22**, 159-172. http://doi.10.5853/jos.2019.02978 2020.
4. Koh SH,Park HH. Neurogenesis in Stroke Recovery. *Transl Stroke Res* **8**, 3-13. http://doi.10.1007/s12975-016-0460-z 2017.
5. Rodrigo R*, et al*. Oxidative stress and pathophysiology of ischemic stroke: novel therapeutic opportunities. *CNS Neurol Disord Drug Targets* **12**, 698-714. http://doi.10.2174/18715273113120500015 2013.
6. Wang Y*, et al*. A review of the relationship between long noncoding RNA and post-stroke injury repair. *J Int Med Res* **47**, 4619-4624. http://doi.10.1177/0300060519867493 2019.
7. Ren W,Yang X. Pathophysiology of Long Non-coding RNAs in Ischemic Stroke. *Front Mol Neurosci* **11**, 96. http://doi.10.3389/fnmol.2018.00096 2018.
8. Alishahi M*, et al*. Long non-coding RNAs and cell death following ischemic stroke. *Metab Brain Dis* **34**, 1243-1251. http://doi.10.1007/s11011-019-00423-2 2019.
9. Yang L,Lu ZN. Long non-coding RNA HOTAIR promotes ischemic infarct induced by hypoxia through up-regulating the expression of NOX2. *Biochem Biophys Res Commun* **479**, 186-191. http://doi.10.1016/j.bbrc.2016.09.023 2016.
10. Sun Y,Hu ZQ. LncRNA HOTAIR aggravates myocardial ischemia-reperfusion injury by sponging microRNA-126 to upregulate SRSF1. *Eur Rev Med Pharmacol Sci* **24**, 9046-9054. http://doi.10.26355/eurrev_202009_22850 2020.
11. Yan H*, et al*. Long non-coding RNA MEG3 functions as a competing endogenous RNA to regulate ischemic neuronal death by targeting miR-21/PDCD4 signaling pathway. *Cell Death Dis* **8**, 3211. http://doi.10.1038/s41419-017-0047-y 2017.
12. Lin Q, Hou S, Dai Y, Jiang N,Lin Y. LncRNA HOTAIR targets miR-126-5p to promote the progression of Parkinson's disease through RAB3IP. *Biol Chem* **400**, 1217-1228. http://doi.10.1515/hsz-2018-0431 2019.
13. Eyileten C*, et al*. MicroRNAs as Diagnostic and Prognostic Biomarkers in Ischemic Stroke-A Comprehensive Review and Bioinformatic Analysis. *Cells* **7**, http://doi.10.3390/cells7120249 2018.
14. Yin KJ, Hamblin M,Chen YE. Angiogenesis-regulating microRNAs and Ischemic Stroke. *Curr Vasc Pharmacol* **13**, 352-365. http://doi.10.2174/15701611113119990016 2015.
15. Jickling GC, Ander BP, Zhan X, Noblett D, Stamova B,Liu D. microRNA expression in peripheral blood cells following acute ischemic stroke and their predicted gene targets. *PLoS One* **9**, e99283. http://doi.10.1371/journal.pone.0099283 2014.
16. Zheng D*, et al*. Role of miR-148a in Mitigating Hepatic Ischemia-Reperfusion Injury by Repressing the TLR4 Signaling Pathway via Targeting CaMKIIalpha in Vivo and in Vitro. *Cell Physiol Biochem* **49**, 2060-2072. http://doi.10.1159/000493716 2018.

17. Zeng J*, et al*. Metformin Protects against Oxidative Stress Injury Induced by Ischemia/Reperfusion via Regulation of the lncRNA-H19/miR-148a-3p/Rock2 Axis. *Oxid Med Cell Longev* **2019**, 8768327. http://doi.10.1155/2019/8768327 2019.
18. Clausen BH*, et al*. Fumarate decreases edema volume and improves functional outcome after experimental stroke. *Exp Neurol* **295**, 144-154. http://doi.10.1016/j.expneurol.2017.06.011 2017.
19. Wang LH*, et al*. CELSR1 Promotes Neuroprotection in Cerebral Ischemic Injury Mainly Through the Wnt/PKC Signaling Pathway. *Int J Mol Sci* **21**, http://doi.10.3390/ijms21041267 2020.
20. Chen J*, et al*. Therapeutic benefit of intravenous administration of bone marrow stromal cells after cerebral ischemia in rats. *Stroke* **32**, 1005-1011. http://doi.10.1161/01.str.32.4.1005 2001.
21. Lowry NC, Pardon LP, Yates MA,Juraska JM. Effects of long-term treatment with 17 beta-estradiol and medroxyprogesterone acetate on water maze performance in middle aged female rats. *Horm Behav* **58**, 200-207. http://doi.10.1016/j.yhbeh.2010.03.018 2010.
22. Zhang X, Liu Z, Shu Q, Yuan S, Xing Z,Song J. LncRNA SNHG6 functions as a ceRNA to regulate neuronal cell apoptosis by modulating miR-181c-5p/BIM signalling in ischaemic stroke. *J Cell Mol Med* **23**, 6120-6130. http://doi.10.1111/jcmm.14480 2019.
23. Fan T*, et al*. An improved method for primary culture of normal cervical epithelial cells and establishment of cell model in vitro with HPV-16 E6 gene by lentivirus. *J Cell Physiol* **233**, 2773-2780. http://doi.10.1002/jcp.25978 2018.
24. Miranda KC*, et al*. A pattern-based method for the identification of MicroRNA binding sites and their corresponding heteroduplexes. *Cell* **126**, 1203-1217. http://doi.10.1016/j.cell.2006.07.031 2006.
25. Li JH, Liu S, Zhou H, Qu LH,Yang JH. starBase v2.0: decoding miRNA-ceRNA, miRNA-ncRNA and protein-RNA interaction networks from large-scale CLIP-Seq data. *Nucleic Acids Res* **42**, D92-97. http://doi.10.1093/nar/gkt1248 2014.
26. Yan G, Zhao H,Hong X. LncRNA MACC1-AS1 attenuates microvascular endothelial cell injury and promotes angiogenesis under hypoxic conditions via modulating miR-6867-5p/TWIST1 in human brain microvascular endothelial cells. *Ann Transl Med* **8**, 876. http://doi.10.21037/atm-20-4915 2020.
27. Marques BL*, et al*. The role of neurogenesis in neurorepair after ischemic stroke. *Semin Cell Dev Biol* **95**, 98-110. http://doi.10.1016/j.semcdb.2018.12.003 2019.
28. Bao Z, Yang Z, Huang Z, Zhou Y, Cui Q,Dong D. LncRNADisease 2.0: an updated database of long non-coding RNA-associated diseases. *Nucleic Acids Res* **47**, D1034-D1037. http://doi.10.1093/nar/gky905 2019.
29. Satani N,Savitz SI. Is Immunomodulation a Principal Mechanism Underlying How Cell-Based Therapies Enhance Stroke Recovery? *Neurotherapeutics* **13**, 775-782. http://doi.10.1007/s13311-016-0468-9 2016.
30. Tobin MK, Bonds JA, Minshall RD, Pelligrino DA, Testai FD,Lazarov O. Neurogenesis and inflammation after ischemic stroke: what is known and where we go from here. *J Cereb Blood Flow Metab* **34**, 1573-1584. http://doi.10.1038/jcbfm.2014.130 2014.

31. Peng CL, Zhao XJ, Wei CC,Wu JW. LncRNA HOTAIR promotes colon cancer development by down-regulating miRNA-34a. *Eur Rev Med Pharmacol Sci* **23**, 5752-5761. http://doi.10.26355/eurrev_201907_18312 2019.
32. Chen D*, et al*. Pyruvate Kinase M2 Increases Angiogenesis, Neurogenesis, and Functional Recovery Mediated by Upregulation of STAT3 and Focal Adhesion Kinase Activities After Ischemic Stroke in Adult Mice. *Neurotherapeutics* **15**, 770-784. http://doi.10.1007/s13311-018-0635-2 2018.
33. Goodman WA*, et al*. KLF6 contributes to myeloid cell plasticity in the pathogenesis of intestinal inflammation. *Mucosal Immunol* **9**, 1250-1262. http://doi.10.1038/mi.2016.1 2016.
34. Zhang X*, et al*. LncRNA-1810034E14Rik reduces microglia activation in experimental ischemic stroke. *J Neuroinflammation* **16**, 75. http://doi.10.1186/s12974-019-1464-x 2019.
35. Chen Z*, et al*. Mitochondrial E3 ligase MARCH5 regulates FUNDC1 to fine-tune hypoxic mitophagy. *EMBO Rep* **18**, 495-509. http://doi.10.15252/embr.201643309 2017.
36. Zhao J, Li H,Chang N. LncRNA HOTAIR promotes MPP+-induced neuronal injury in Parkinson's disease by regulating the miR-874-5p/ATG10 axis. *EXCLI J* **19**, 1141-1153. http://doi.10.17179/excli2020-2286 2020.
37. Li K, Lin T, Chen L,Wang N. MicroRNA-93 elevation after myocardial infarction is cardiac protective. *Med Hypotheses* **106**, 23-25. http://doi.10.1016/j.mehy.2017.07.003 2017.
38. Liu J, Huang GQ,Ke ZP. Silence of long intergenic noncoding RNA HOTAIR ameliorates oxidative stress and inflammation response in ox-LDL-treated human macrophages by upregulating miR-330-5p. *J Cell Physiol* **234**, 5134-5142. http://doi.10.1002/jcp.27317 2019.
39. Lu W, Zhu L, Ruan ZB, Wang MX, Ren Y,Li W. HOTAIR promotes inflammatory response after acute myocardium infarction by upregulating RAGE. *Eur Rev Med Pharmacol Sci* **22**, 7423-7430. http://doi.10.26355/eurrev_201811_16282 2018.
40. Xia H*, et al*. Andrographolide antagonizes the cigarette smoke-induced epithelial-mesenchymal transition and pulmonary dysfunction through anti-inflammatory inhibiting HOTAIR. *Toxicology* **422**, 84-94. http://doi.10.1016/j.tox.2019.05.009 2019.
41. Liu XH*, et al*. Lnc RNA HOTAIR functions as a competing endogenous RNA to regulate HER2 expression by sponging miR-331-3p in gastric cancer. *Mol Cancer* **13**, 92. http://doi.10.1186/1476-4598-13-92 2014.
42. Patel V*, et al*. The stretch responsive microRNA miR-148a-3p is a novel repressor of IKBKB, NF-kappaB signaling, and inflammatory gene expression in human aortic valve cells. *FASEB J* **29**, 1859-1868. http://doi.10.1096/fj.14-257808 2015.
43. Zheng D, He D, Lu X, Sun C, Luo Q,Wu Z. [The miR-148a alleviates hepatic ischemia/reperfusion injury in mice via targeting CaMKIIalpha]. *Xi Bao Yu Fen Zi Mian Yi Xue Za Zhi* **32**, 1202-1206. 2016.
44. Syafruddin SE, Mohtar MA, Wan Mohamad Nazarie WF,Low TY. Two Sides of the Same Coin: The Roles of KLF6 in Physiology and Pathophysiology. *Biomolecules* **10**, http://doi.10.3390/biom10101378 2020.

45. Zhang Y, *et al*. MiR-181d-5p Targets KLF6 to Improve Ischemia/Reperfusion-Induced AKI Through Effects on Renal Function, Apoptosis, and Inflammation. *Front Physiol* **11**, 510. http://doi.10.3389/fphys.2020.00510 2020.
46. Kim GD, Ng HP, Chan ER,Mahabeleshwar GH. Kruppel-like factor 6 promotes macrophage inflammatory and hypoxia response. *FASEB J* **34**, 3209-3223. http://doi.10.1096/fj.201902221R 2020.
47. Wang Z, *et al*. KLF6 and STAT3 co-occupy regulatory DNA and functionally synergize to promote axon growth in CNS neurons. *Sci Rep* **8**, 12565. http://doi.10.1038/s41598-018-31101-5 2018.
48. Liu ZJ, *et al*. Melatonin protects against ischemic stroke by modulating microglia/macrophage polarization toward anti-inflammatory phenotype through STAT3 pathway. *CNS Neurosci Ther* **25**, 1353-1362. http://doi.10.1111/cns.13261 2019.
49. Li Y, *et al*. Salvianolic acids enhance cerebral angiogenesis and neurological recovery by activating JAK2/STAT3 signaling pathway after ischemic stroke in mice. *J Neurochem* **143**, 87-99. http://doi.10.1111/jnc.14140 2017.
50. Cheng D, *et al*. LncRNA HOTAIR epigenetically suppresses miR-122 expression in hepatocellular carcinoma via DNA methylation. *EBioMedicine* **36**, 159-170. http://doi.10.1016/j.ebiom.2018.08.055 2018.

Figures

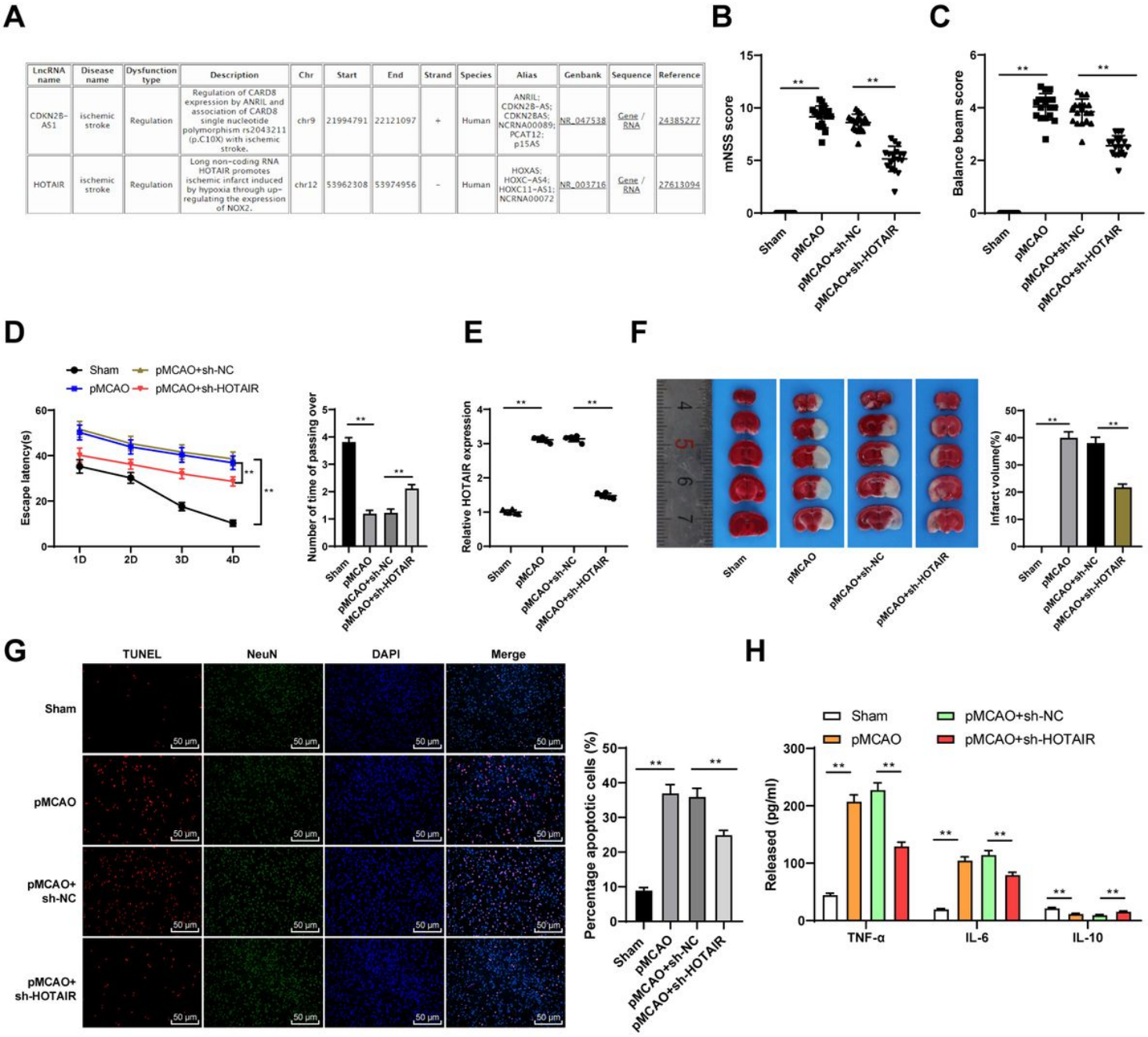

LncRNA name	Disease name	Dysfunction type	Description	Chr	Start	End	Strand	Species	Alias	Genbank	Sequence	Reference
CDKN2B-AS1	ischemic stroke	Regulation	Regulation of CARD8 expression by ANRIL and association of CARD8 single nucleotide polymorphism rs2043211 (p.C10X) with ischemic stroke.	chr9	21994791	22121097	+	Human	ANRIL; CDKN2B-AS; CDKN2BAS; NCRNA00089; PCAT12; p15AS	NR_047538	Gene / RNA	24385277
HOTAIR	ischemic stroke	Regulation	Long non-coding RNA HOTAIR promotes ischemic infarct induced by hypoxia through up-regulating the expression of NOX2.	chr12	53962308	53974956	-	Human	HOXAS; HOXC-AS4; HOXC11-AS1; NCRNA00072	NR_003716	Gene / RNA	27613094

Figure 1

LncRNA HOTAIR inhibited recovery of neurological function in pMCAO mice. A: retrieval of Ischemic stroke related lncRNAs; pMCAO mouse model was established and injected wtih shRNA HOTAIR into the right side of brain with shRNA NC as control; B: neurologic score evaluated using mNSS method, N = 18; C: beam balance test, N = 18; D: Morris water maze test; E: expression of HOTAIR was detected by RT-qPCR after 24 h of pMCAO; F: TTC staining and cerebral infarcted area; G: cerebral cell apoptosis was detected by TUNEL staining; H: levels of inflammatory cytokines (TNF-α, IL-6, and IL-10) were measured by ELISA, N = 6. Data are presented as the means ± SD. Data in panels B-C and E-G were analyzed using one-way ANOVA, followed by Tukey's multiple comparisons test or Sidak's multiple comparisons test.

Data in panels D and H were analyzed using two-way ANOVA, followed by Tukey's multiple comparisons test, **P < 0.01.

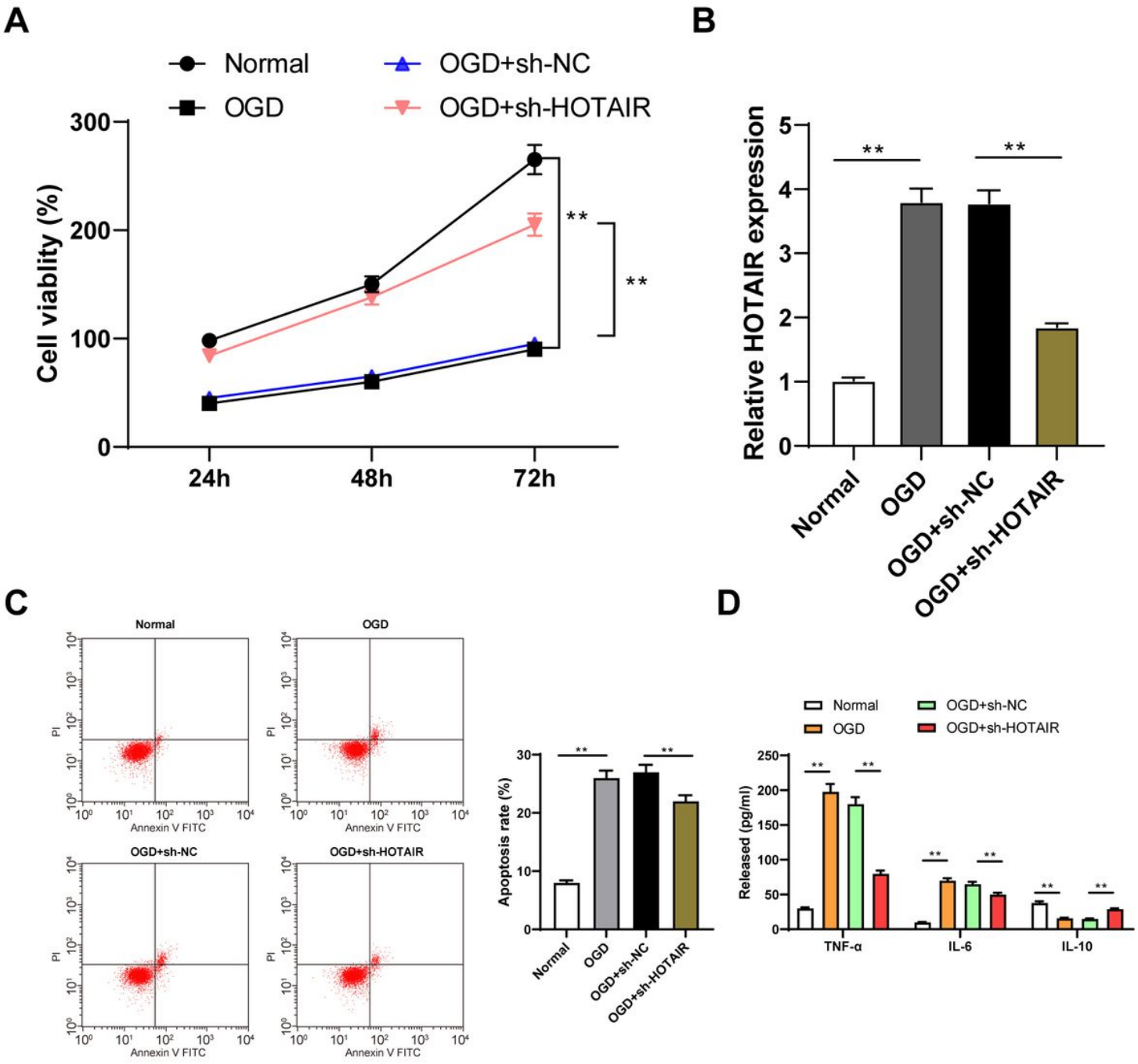

Figure 2

Silencing HOTAIR promoted viability of OGD-injured N2a cells and attenuated apoptosis and inflammation. OGD model using N2a cells was established. N2a cells were infected by shRNA HOTAIR with shRNA NC as control. A: viability of OGD-induced N2a cells was detected by CCK-8; B: the expression of HOTAIR in OGD-induced N2a cells was detected by RT-qPCR; C: apoptosis was determined by flow cytometry; D: levels of inflammatory cytokines (TNF-α, IL-6, and IL-10) in OGD-induced N2a cells were measured by ELISA. The experiment was repeated 3 times independently. Data are presented as the

means ± SD. Data in panels A and D were analyzed using two-way ANOVA while data in panels B and C using one-way ANOVA, followed by Tukey's multiple comparisons test, **P < 0.01.

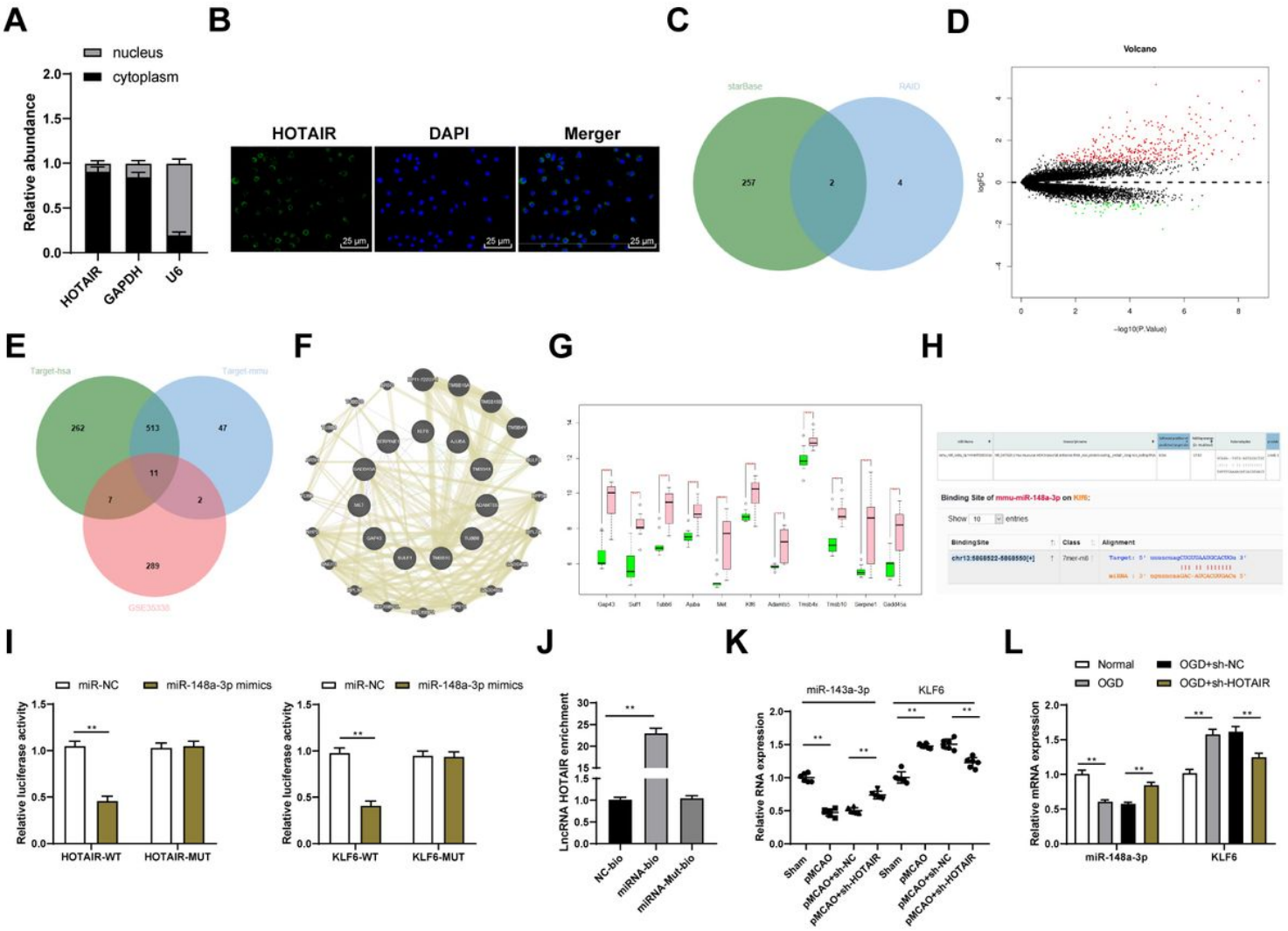

Figure 3

HOTAIR regulated KLF6 expression via targeting miR-148a-3p. A: LncATLAS predicted that HOTAIR was located in cytoplasm; B: fractionation of nuclear and cytoplasmic RNA; C: the distribution of lncRNA HOTAIR in OGD-induced N2a cells was determined by FISH; D: interaction of HOTAIR and miRs was predicted by starBase and RAID databases. The two circles represented the predicted results and the intersection of the two sets of data lied in the middle; E: volcano plot of differentially expressed genes in GSE35338 chip, with -log10pval as abscissa and logFC as ordinate. The red dots represented highly expressed genes in IS while green dots represented lowly expressed genes; F: target genes of miR-148a-3p in human and mice predicted by TargetScan database and the intersection with up-regulated genes in GSE35338. The intersection was presented in the middle; G: interaction analysis of 11 target genes of miR-148a-3p with each circle representing a gene and lines representing the interaction. Candidate target genes were located in the middle, surrounded by 20 relative genes predicted by GeneMANIA database; H: differential expression of 11 candidate target genes in GSE35338 chip with gene as abscissa and

expression value as ordinate, and green box representing normal samples, red box representing IS samples; I: binding sites of lncRNA HOTAIR and miR-148a-3p, and binding sites of miR-148a-3p and KLF6 were predicted by RNA22 v2 and starBase; J: dual-luciferase reporter assay revealed that HOTAIR targeted miR-148a-3p, and miR-148a-3p targeted KLF6; K: RNA pull-down; L-M: The levels of miR-148a-3p and KLF6 in mice or cells overexpressing HOTAIR were detected by RT-qPCR. The cell experiment was repeated 3 times independently. Data are presented as the means ± SD. Data in panel K were analyzed using one-way ANOVA, and data in panels B, J and L-M were analyzed using two-way ANOVA, followed by Tukey's multiple comparisons test or Sidak's multiple comparisons test, **P < 0.01, ***P < 0.001.

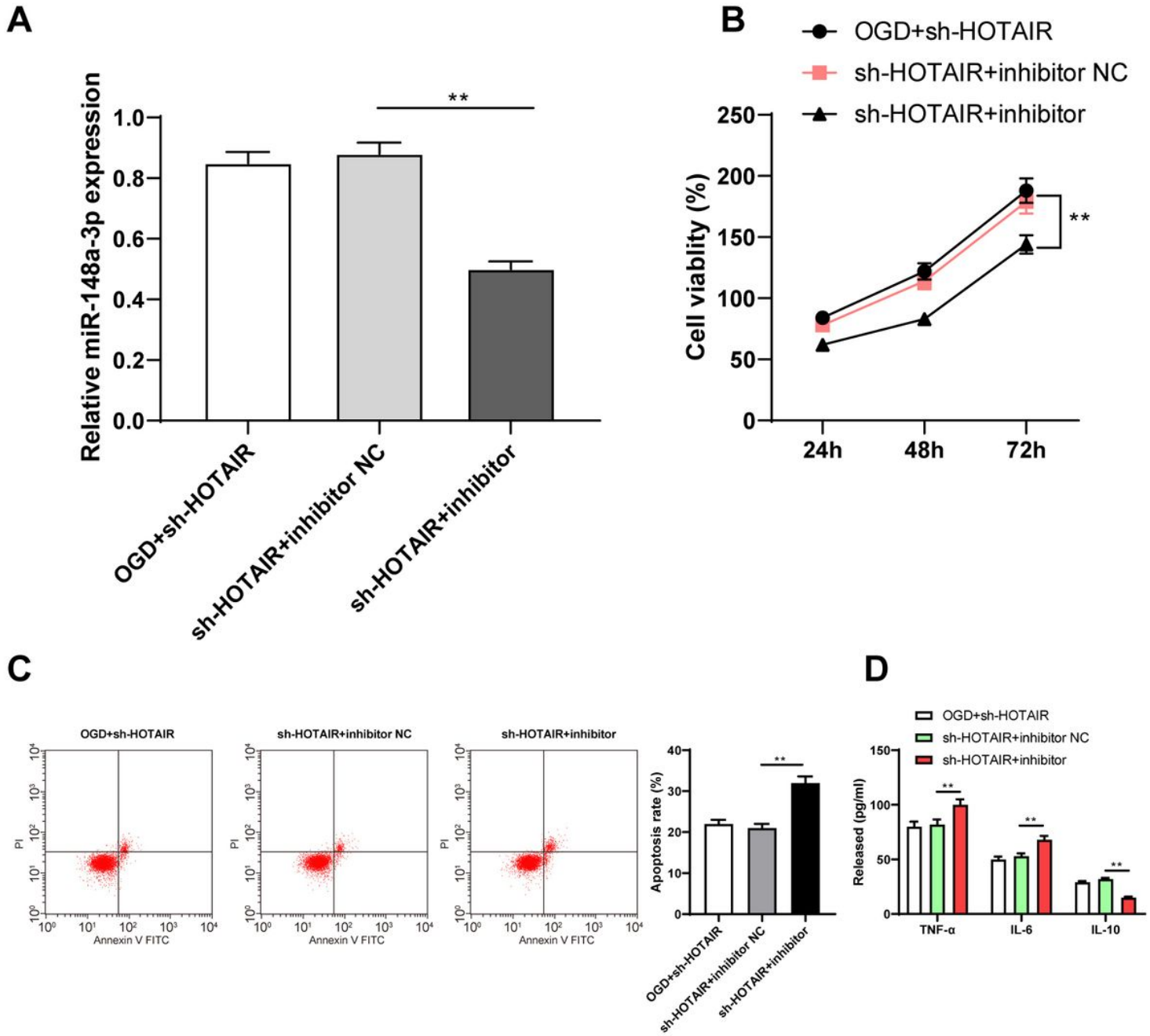

Figure 4

miR-148a-3p downregulation partially reversed the effect of sh-HOTAIR on N2a cells post-ischemia. miR-148a-3p inhibitor was transferred to N2a cells with silencing HOTAIR, with transfection of inhibitor NC as control. And then N2a cells were induced by OGD. A: expression of miR-148a-3p was detected by RT-qPCR; B: cell viability was determined by CCK-8; C: apoptosis was determined by flow cytometry; D: levels of inflammatory cytokines (TNF-α, IL-6, and IL-10) were measured by ELISA. The cell experiment was repeated 3 times independently. Data are presented as the means ± SD. Data in panels A and D were analyzed using one-way ANOVA, and data in panels B and D were analyzed using two-way ANOVA, followed by Tukey's multiple comparisons test, **P < 0.01.

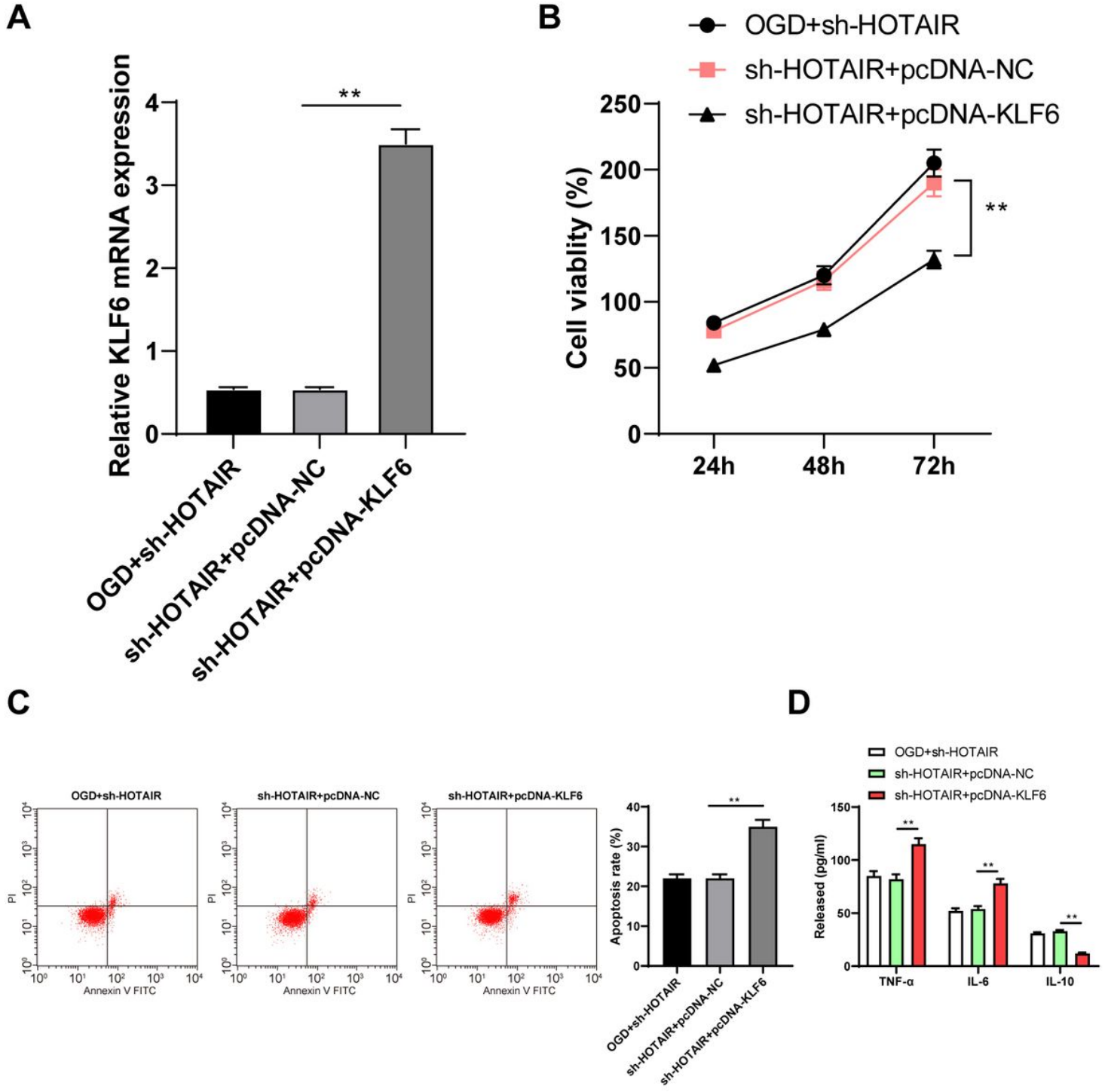

Figure 5

KLF6 overexpression suppressed the effect of silencing HOTAIR on OGD-induced cell injury. pcDNA-KLF6 was transferred into cells silencing HOTAIR, with transfection of pcDNA-NC as control, and then cells were induced by OGD. A: KLF6 expression was detected by RT-qPCR; B: cell viability was determined by CCK-8; C: apoptosis was determined by flow cytometry; D: levels of inflammatory cytokines (TNF-α, IL-6, and IL-10) were measured by ELISA. The cell experiment was repeated 3 times independently. Data are presented as the means ± SD. Data in panels A and C were analyzed using one-way ANOVA and data in panels B and D were analyzed using two-way ANOVA, followed by Tukey's multiple comparisons test, **P < 0.01.

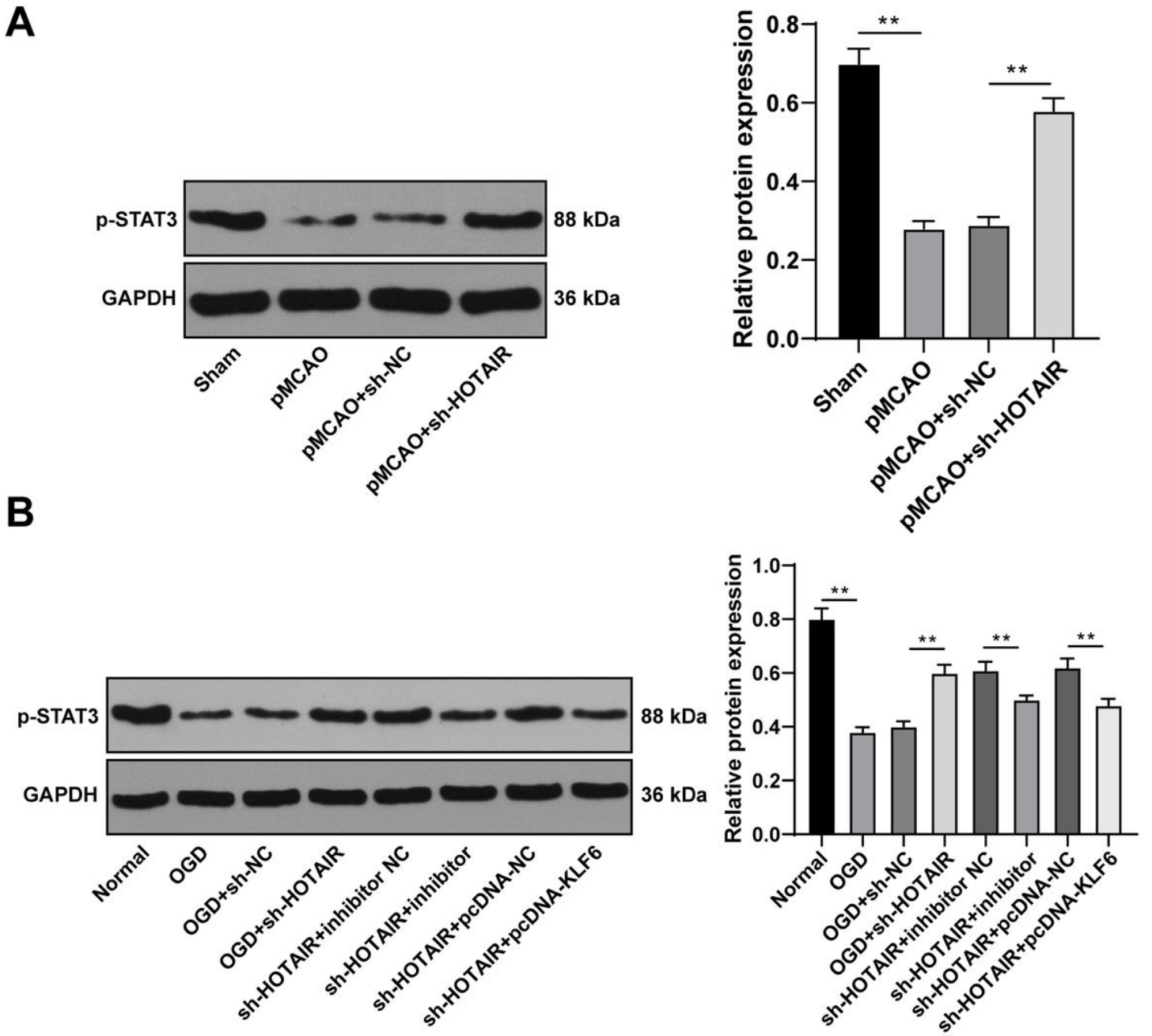

Figure 6

HOTAIR blocked the activation of STAT3 signaling pathway via miR-148a-3p/KLF6. A: Western blot was used to detect levels of p-STAT3 protein in pMCAO model, N = 6; B: Western blot was used to detect levels of p-STAT3 protein in OGD-induced N2a cells. The cell experiment was repeated 3 times independently. Data are presented as the means ± SD. All data were analyzed using one-way ANOVA, followed by Sidak's multiple comparisons test, **P < 0.01.

Supplementary Files

This is a list of supplementary files associated with this preprint. Click to download.

- originalfigure6A.jpg
- originalfigure6B.jpg
- SupplementaryTable1.docx